Field Orientation Control of a Wind Driven DFIG Connected to the Grid

MAHMOUD A. MOSSA
Electrical Engineering Department, Faculty of Engineering
El-Minia University
EL- Minia, Egypt, 61111
EGYPT
eng_mahmoud2015@yahoo.com

Abstract:-This paper aims to develop a method of field orientation scheme for controlling both active and reactive powers of a DFIG (double fed induction generator) driven by a wind turbine. The controlled system consists of a wind turbine that drives a DFIG connected to the utility grid through AC-DC-AC link. The control method is based on the theory of controlling the d^e and q^e axes components of voltage and current for both rotor side and line side converters using PI controllers. The main control objective is to regulate the dc link voltage for operating at the maximum available wind power. A mathematical dynamic model of a DFIG driven by a wind turbine system is presented. Digital simulation has been carried out in order to evaluate the effectiveness of the proposed system. The results confirm that good steady state and dynamic performances of the proposed system has been achieved under different types of wind speed variations.

Key-Words: - Wind turbine, DFIG, reactive power control of induction machines, PI controller, field orientation, WECS, MATLAB simulation.

List of symbols

V_{ds}^e, V_{qs}^e d^e-axis and q^e -axis stator voltages.

i_{ds}^e, i_{qs}^e d^e-axis and q^e-axis stator currents**.**

V_{dr}^e, V_{qr}^e d^e-axis and q^e-axis rotor voltages**.**

i_{dr}^e, i_{qr}^e d^e-axis and q^e-axis rotor currents.

i_{md}^e, i_{mq}^e d^e-axis and q^e-axis magnetizing currents.

V_{ds}^s, V_{qs}^s d^s-axis and q^s -axis stator voltages.

i_{ds}^s, i_{qs}^s d^s-axis and q^s-axis stator currents**.**

i_{dr}^s, i_{qr}^s d^s-axis and q^s-axis rotor currents.

R_s stator winding resistance, Ω.

R_r rotor winding resistance, Ω.
L_m magnetizing inductance, H.
L_s stator self inductance, H.
L_r rotor self inductance, H.
L_{ls} stator leakage inductance, H.
L_{lr} rotor leakage inductance, H.
ω_r electrical rotor angular speed in rad./sec.
V_w wind speed, m./sec.
p d/dt, the differential operator.
T_m mechanical torque in the shaft, N.m.
T_e electromagnetic torque, N.m.
B friction damping coefficient, N.m./rad./sec.
J_m machine moment of inertia, Kg.m^2.
P_s, Q_s stator active and reactive power.
P_m turbine power, W.
P number of pole pairs.
θ_e electrical stator flux angle, degree.
θ_r electrical rotor angular position, degree.
θ_{slip} electrical slip flux angle, degree.
β blade pitch angle, degree.
μ ratio of the rotor blade tip speed and wind speed.
ρ specific density of the air, Kg.m^3.
A swept area of the blades, m^2.
$C_p(\beta, \mu)$ turbine power coefficient.
D_r rotor diameter in meters.

Subscripts

d-q direct and quadrature axis.
s,r stator and rotor, respectively.
* denote the reference value.
^ denote the estimated value.

1 Introduction

Wind electrical power system are recently getting lot of attention, because they are cost competitive, environmental clean and safe renewable power sources, as compared with fossil fuel and nuclear power generation. A special type of induction generator, called a doubly fed induction generator (DFIG), is used extensively for high-power wind applications [1]. They are used more and more in wind turbine applications due to ease controllability, high energy efficiency and improved power quality.

Fixed speed generators and induction generators had the disadvantage of having low power efficiencies at most

speeds. Turbines are commonly installed in rural areas with unbalanced power transmission grids [2] and [3]. For an induction machine an unbalanced grid imposes negative effects like overheating and mechanical stress due to torque pulsations.

For example for an unbalance of about 6% the induction generator is stopped from generating to the grid. By control of the rotor currents of a DFIG, the effects of unbalanced stator voltages may be compensated for. DFIG's ability to control rotor currents, allows for reactive power control and variable speed operation, so it can operate at maximum efficiency over a wide range of wind speeds [4] and [5]. The doubly-Fed Induction Generator (DFIG) is widely used for variable-speed generation and it is one of the most important generators for wind energy conversion systems (WECS).

Various control strategies have been proposed for regulating grid voltage and / or achieving optimal output of the turbine. In some schemes, the wind turbine drives a DFIG connected to the grid through a static converter [6]. Other control schemes use search methods that vary the speed until optimal generator output power is obtained [7]. However, these techniques have the difficulty of tracking the wind speed, which causes additional stress on the shaft.

Recently, advanced control techniques, which were applied successfully on the machine drives, have been proposed for regulating the wind power in a grid connected wind energy conversion scheme. They include variable structure control [8], direct power control using space vector modulation [9], fuzzy control, and field orientation control [10]. In these methods, the speed feedback may be necessary to avoid instability. In this paper there is no need for speed sensor as the stator flux and rotor flux phase angles are directly calculated from the stator flux and rotor flux linkages respectively.

This paper aims to develop a method of field orientation scheme for control of both active and reactive powers of a DFIG driven by a wind turbine. The controlled system consists of a wind turbine that drives a DFIG connected to the utility grid through AC-DC-AC link. The control method is based on the theory of controlling the d^e and q^e axes components of voltage and current for both rotor side and line side converters using PI controllers. The main control objective is to regulate the dc link voltage for operation at maximum available wind power. Using MATLAB/SIMULINK software, the performances of the proposed system are evaluated during the variation of wind speed. This paper describes the complete dynamic model of the proposed system and explains the field oriented control of a DFIG. Computer simulations have been carried out in order to validate the effectiveness of the proposed system. The results prove that , better overall performances are achieved regarding to high estimation accuracy, quick recover from wind speed disturbance in addition to good tracking ability.

2 System Description

Fig.1 shows a basic layout of a DFIG driven by a wind turbine system. The machine may be simulated as an induction machine having 3-phase supply on the stator and three phase supply on the rotor. The rotor circuit is

connected through slip rings to the back to back converters arrangement controlled by pulse width modulation (PWM) strategies [10] and [11]. The ratings of these converters for speed range of operation are restricted to a fraction of the machine rated power.

The voltage magnitude and power direction between the rotor and the supply may be varied by controlling the switch impulses, which drive the IGBTs inverter. Back to back converters consist of two voltage source converters (ac-dc-ac) having a dc link capacitor connecting them. The generator side converter takes the variable frequency voltage and converts it into a dc voltage. The grid side converter has the voltage conversion from the dc link as input and ac voltage at grid as output. Rotor-side converter acts as a voltage source converter, while the grid-side convertor is expected to keep the capacitor voltage constant under wind speed variations and at different operating conditions of the grid [12] and [13]. The current and voltage controllers of Figure1 are included for obtaining the rotor side and line side voltage references (V^*_{abcr} and V^*_{abcl}).

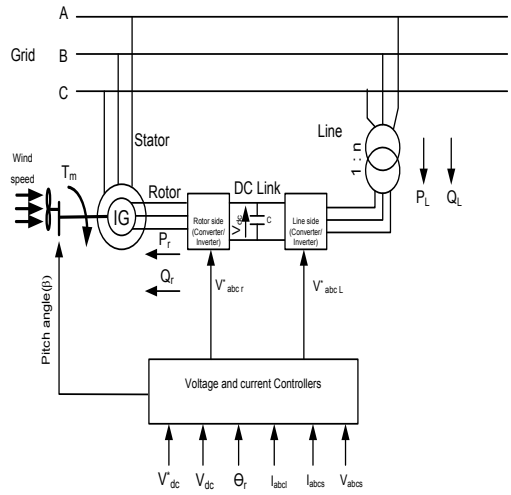

Fig. 1: Doubly-fed induction Generator driven by a wind turbine System

3 Dynamic Modeling of the DFIG

3.1 Turbine model

To operate a wind turbine at its optimum power output at different wind speeds, the wind turbine should be operated at its maximum power coefficient ($C_p(\beta,\mu)_{,\ optimum}$= 0.3-0.5). The wind turbine should be operated at a constant tip-speed ratio (μ) for operation around its maximum power coefficient [14]. As the wind speed increases, the rotor speed should follow the variation of the wind speed [15]. In general, the load on the wind turbine is regulated as a cube function of the wind speed to operate the wind turbine at the optimum efficiency. The aerodynamic power generated by wind turbine can be written as [15]:

$$P_m = 0.5\rho A V_w^3 C_p(\beta,\mu) \qquad (1)$$

Where the turbine power coefficient is defined in terms of the ratio of the

rotor blade tip speed (μ) and the blade pitch angle (β) as [16]:

$$C_p(\beta,\mu) = 0.73\left(\frac{151}{\mu} - 0.002 - 13.2\right)e^{\frac{-18.4}{\mu}}$$

Where

$$\mu = \frac{D_r \omega_r}{2V_w}$$

At lower wind speed, the blade pitch angle is set to a null value, because, the maximum power coefficient is obtained for this angle. Pitch angle control operates only when the value for wind speed is greater than the nominal wind speed [14].

To track the wind speed precisely, the power can also be expressed in terms of the rotor speed. In reality, the wind turbine rotor has a significantly large inertia due to the blade inertia and other rotating components.

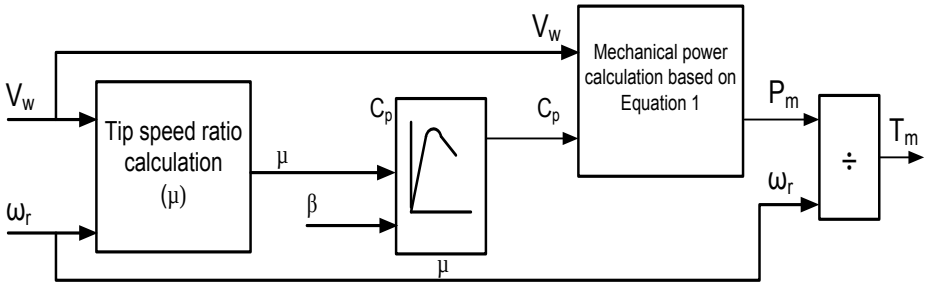

Fig. 2: Wind turbine control system

Fig.2 shows the wind turbine control system. The inputs to block are turbine speed (ω_r), blade pitch angle (μ) and wind speed (V_w). The turbine speed is obtained from the power-speed characteristics curve (tracking characteristics) [15]. the mechanical torque on the shaft is calculated as:

$$T_m = \frac{P_m}{\omega_r} \qquad (2)$$

3.2 Induction machine model

The general equations for the d^s-q^s representation of an induction machine, in the stationary stator reference frame, are given as [16]:

$$\begin{bmatrix} V_{ds}^s \\ V_{qs}^s \\ V_{dr}^s \\ V_{qr}^s \end{bmatrix} = \begin{bmatrix} R_s + pL_s & 0 & pL_m & 0 \\ 0 & R_s + pL_s & 0 & pL_m \\ pL_m & \omega_r L_m & R_r + pL_r & \omega_r L_r \\ -\omega_r L_m & pL_m & -\omega_r L_r & R_r + pL_r \end{bmatrix} \begin{bmatrix} i_{ds}^s \\ i_{qs}^s \\ i_{dr}^s \\ i_{qr}^s \end{bmatrix} \qquad (3)$$

The developed electromagnetic torque in terms of stator and rotor current components can be expressed as:

$$T_e = \frac{3}{2}\frac{P}{2}L_m(i_{qs}^s i_{dr}^s - i_{ds}^s i_{qr}^s) \quad (4)$$

The mechanical equation in the generating region is given as:

$$T_m = J_m p\omega_r + B\omega_r + T_e \quad (5)$$

The state-space form of equation (5) can be written as:

$$p\omega_r = \frac{T_m - T_e - B\omega_r}{J_m} \quad (6)$$

3.3 DC link model

Fig.3 shows the blocked diagram of the dc link model, which consists of the line side and rotor side converters and the dc link capacitor. The dc link capacitor provides dc voltage to the rotor side converter and any attempt to store reactive power in the capacitor would raise its voltage level [9]. To ensure stability of the system, power flow of the line side and rotor side converters, as indicated in fig. 3, should guarantee the following control objective:

$$P_L = P_r \quad (7)$$

The differential equation of the dc link can be written as:

$$pcV_{dc} = i_1 - i_2 \quad (8)$$

Where V_{dc} is the dc voltage at the converter output terminals and c is the smoothing capacitor. Assuming no power losses for the converters, i_1 and i_2 can be derived as

$$i_1 = \frac{P_L}{V_{dc}} \quad (9)$$

$$i_2 = \frac{P_r}{V_{dc}} \quad (10)$$

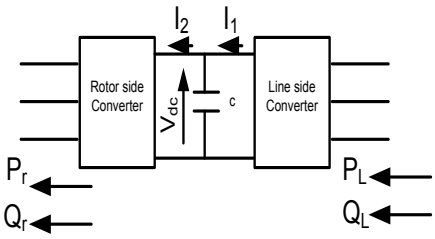

Fig.3: Power flow through dc-link element

4 Complete System Model

The above subsystem dynamic models can be interfaced to form the unified nonlinear dynamic model of the wind generation system. The system can be described by the following differential equations:

$$pi_{ds}^s = A_2\omega_r L_m i_{qs}^s - R_s A_1 i_{ds}^s + R_r A_2 i_{dr}^s + A_1\omega_r L_m i_{qr}^s - A_1 V_{ds}^s \quad (11)$$

$$pi_{qs}^s = A_1 V_{qs}^s - R_s A_1 i_{qs}^s - A_2\omega_r L_m i_{ds}^s + R_r A_2 i_{qr}^s - A_1\omega_r L_r i_{dr}^s \quad (12)$$

$$pi_{dr}^s = -A_2\omega_r L_m i_{qs}^s + R_s A_2 i_{ds}^s - A_1\omega_r L_s i_{qr}^s - A_3 i_{dr}^s + A_2 V_{ds}^s \quad (13)$$

$$pi_{qr}^s = R_s A_2 i_{qs}^s + A_2\omega_r L_s i_{ds}^s - A_3 i_{qr}^s + A_1\omega_r L_s i_{dr}^s \quad (14)$$

Where $A_1 = \frac{L_r}{(L_s L_r - L_m^2)}$,

$A_2 = \frac{L_m}{(L_s L_r - L_m^2)}$, and

$A_3 = \frac{R_r(1 + A_2 L_m)}{L_r}$

$$p\omega_r = \frac{1}{J_m}[T_m - B\omega_r - \frac{3}{2}\frac{P}{2}L_m(i_{qs}^s i_{dr}^s - i_{ds}^s i_{qr}^s)] \quad (15)$$

$$pcV_{dc} = \frac{P_L}{V_{dc}} - \frac{P_r}{V_{dc}} \quad (16)$$

5 Field Oriented Control of a DFIG

The field orientation techniques allow decoupled or independent control of both active and reactive power. These techniques are based on the concept of d^e-q^e controlling in different reference frames [14] and [15], where the current and the voltage are decomposed into distinct components related to the active and reactive power. In this work, the stator flux oriented rotor current control, with decoupled control of active and reactive powers is adopted.

The control schemes for the doubly-fed induction machine are expected to track a prescribed maximum power curve, for maximum power capturing and to be able to control the reactive power generation. These control objectives must be achieved with adequate stability of the system which also includes the power converter and the dc link. The total active and reactive powers generated can be calculated in terms of d^e-q^e stator voltage and current components as [13]

$$P_s = \frac{3}{2}|V_s| i_{qs}^e \quad (17)$$

$$Q_s = \frac{3}{2}|V_s| i_{ds}^e \quad (18)$$

Where

$$|V_s| = \sqrt{(V_{ds}^e)^2 + (V_{qs}^e)^2}$$

The field orientation control is based on the field d^e-q^e model, where the reference frame rotates synchronously with respect to the stator flux linkage, with the d-axis of the reference frame instantaneously overlaps the axis of the stator flux. By aligning the stator flux phasor λ_s on the d^e- axis, so ($\omega = \omega_e$ and $\lambda_{qs}^e = 0$, $\lambda_{ds}^e = \lambda_s$). In such case the following expressions are obtained

$$\lambda_{qs}^e = L_s i_{qs}^e + L_m i_{qr}^e = 0.0$$

$$\therefore i_{qs}^e = -\frac{L_m}{L_s} i_{qr}^e \quad (19)$$

The developed electromagnetic torque can be expressed in terms of d^e-q^e stator current and flux components as:

$$T_e = \frac{3}{2}\frac{P}{2}(i_{qs}^e \lambda_{ds}^e - i_{ds}^e \lambda_{qs}^e) \quad (20)$$

By putting $\lambda_{qs}^e = 0$, in the torque equation, this yields:

$$\therefore T_e = \frac{3}{2}\frac{P}{2}(i_{qs}^e \lambda_{ds}^e) \quad (21)$$

Using (19) and the active power equation (17), the equation of the active power becomes:

$$P_s = -\frac{3}{2}|V_s|\frac{L_m}{L_s}i_{qr}^e \qquad (22)$$

The d^e-axis stator current component can be written as:

$$i_{ds}^e = i_{md}^e - i_{dr}^e = \frac{|V_s|}{2\pi f_s L_m} - i_{dr}^e \qquad (23)$$

Using (23) and the reactive power equation (18), the equation of the reactive

power can be expressed as follows:

$$Q_s = \frac{3}{2}|V_s|(\frac{|V_s|}{2\pi f_s L_m} - i_{dr}^e) \qquad (24)$$

Therefore, the d^e-axis rotor current component, (i_{dr}^e) can be obtained by regulating the stator reactive power. On the other hand, the q^e–axis rotor current component, (i_{qr}^e) can be obtained by controlling the generated torque which is obtained from the stator active power and the generator speed [15] and [16].

The stator flux linkage components in the stationary stator reference frame can be calculated through the integration of the difference between the phase voltage and the voltage drop in the stator resistance as;

$$\lambda_{ds}^s = \int (V_{ds}^s - i_{ds}^s R_s)dt$$

$$\lambda_{qs}^s = \int (V_{qs}^s - i_{qs}^s R_s)dt \qquad (25)$$

The magnitude of the stator flux linkage and its phase angle are given by:

$$\lambda_s = \sqrt{(\lambda_{ds}^s)^2 + (\lambda_{qs}^s)^2}$$

$$\theta_e = \tan^{-1}\frac{\lambda_{qs}^s}{\lambda_{ds}^s} \qquad (26)$$

6 Complete system configuration

Fig.4 shows the proposed block diagram of the DFIG driven by a wind turbine control system. The control system consists of a reactive power controller, a torque controller, three current controllers, two co-ordinate transformations (C.T), two sinusoidal pulse-width-modulation (SPWM) for transistor bridge converters/inverters, a stator flux and torque estimators and reactive power calculator. The reference value of reactive power, Q_s^*, can be either directly implemented to the converter, considering the appropriate power, or calculated from equation (24).

Individual control of the rotor side converter (RSC), of the line/grid side converter (GSC) and related feedback between the two converters are shown. A sinusoidal pulse width modulator (SPWM) provides field oriented currents i_{dr}^e and i_{qr}^e to the rotor circuit, controlling stator reactive power and electromagnetic torque, respectively. The co-ordinate transformation $(C.T)^{-1}$ in Figure 4 is used for transforming these components to the three phase rotor voltage references by using the field angle.

The control inputs to the (SPWM) are the line voltage or rotor voltage commands and predefined triangular carrier waves. The SPWM modulator calculates the pulse pattern and supplies firing signals to the inverter. In the PWM scheme, the inverter output voltage is defined by the intersections of the voltage commands and carrier waves [17] and [18], which are synchronized such that the carrier

frequency is multiple of the frequency of voltage commands. This manner of synchronization eliminates sub harmonic generation [19]. The reference Torque is given by the turbine optimal torque-speed profile. Another (SPWM) is used to interface with the power network, possibly through a transformer. In the same d^e-q^e reference frame as determined by the stator flux, its currents (i^e_{ql} and i^e_{dl}) are also field oriented, controlling P_L and Q_L, respectively. As discussed earlier, P_L is controlled through i^e_{ql} to stabilize the dc bus voltage and Q_L is controlled through i^e_{dl} to meet the overall reactive power command.

The RSC controls the reactive power (Q) injection and the developed electric power (P_{elec}) given by the DFIG. The electric power reference (P_{opt} *) is determined based on the optimum rotor speed given by the C_p characteristic in Fig.2, depending on the wind speed as a parameter. The calculated reactive power of the DFIG (Q^*) is compared to the estimated one. The reference direct axis current (I^{e*}_{dr}) is then calculated from the resulting (Q) error, through a PI controller. (I^{e*}_{dr}) is then compared to the actual direct axis rotor current (i^e_{dr}), and the error is then sent to another PI controller to determine the reference value of the direct axis rotor voltage (V^{e*}_{dr}).

The quadrature axis component of the rotor current (I^{e*}_{qr}) is calculated in a similar manner as in the direct axis component, and is used to regulates the developed electric power (P_{elec}) to an optimal reference (P_{opt} *). The direct-quadrature components of the reference rotor voltages (V^{e*}_{dr} and V^{e*}_{qr}) are then transformed back into the three-phase voltages (V^*_{abcr}), required at the RSC output, through a dq0-abc transformation. The converters IGBT's are considered to be ideal and commutation losses are therefore neglected.

The GSC controls the voltage level at the direct-current link (DC link) between the two converters. The DC link reference voltage level (V_{dc}*) is set to 1200 V, this voltage is compared to the actual voltage and from the resulting error the direct axis component of the reference line current (I^{e*}_{dl}) is being calculated through a PI controller. (I^{e*}_{dl}) is then compared to the actual value of the direct axis line current (I_{dl}) and then sent to another PI controller, in order to calculate the direct axis reference line voltage (V^{e*}_{dL}).

There is no need for a GSC reactive power regulation, since the RSC already controls the power factor of the DFIG. Therefore the quadrature axis component of the reference current is set to zero ($I^{e*}_{ql} = 0$). I^{e*}_{ql} is then compared to the quadrature axis component of the actual line current (I_{ql}) and the error is sent to a PI controller to determine the quadrature axis component of the reference line voltage (V^{e*}_{qL}). The two components of the reference line voltage (V^{e*}_{dL} and V^{e*}_{qL}) are then transformed into the three-phase voltages (V^*_{abcl}) needed at the output of the GSC.

The method uses the stator reference frame model of the induction machine and the same reference frame is used in the implementation thereby avoiding the trigonometric operations encountered in the C.T of other reference frames. This is one of the advantages of the control scheme.

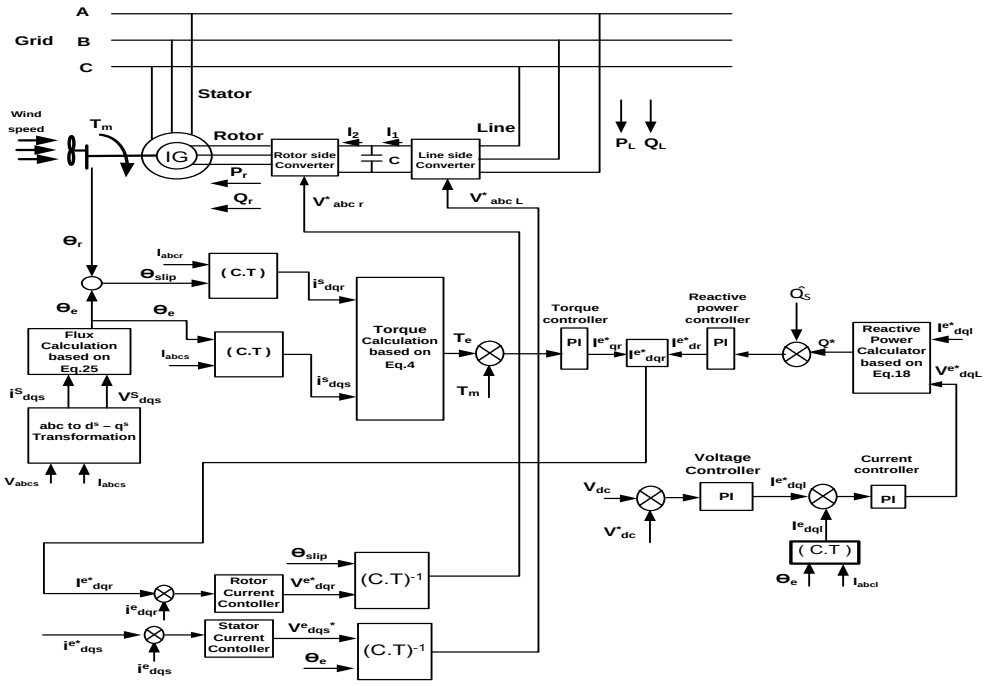

Fig.4: Proposed control scheme of the DFIG driven by a wind turbine based on field orientation.

7 Simulation Results and Discussions

Digital simulation is carried out in order to validate the effectiveness of the proposed scheme of Fig.4. The Matlab/Simulink software package has been used for this purpose. The DFIG under study is a 9 MW, 6-poles, 967 rpm and its nominal parameters and specifications are listed in table1.

Table 1: Parameters and data specifications of the DFIG system.

DFIG and Wind turbine parameters	
P_n(nominal)	9×10^6 W
V_n(rms)	580 V
F_n	50 Hz
R_s	0.104 Ω
R_r	0.0743 Ω
L_{ls}	2.54 (H)
L_{lr}	2.31 (H)
L_m	4.35 (H)
V_{dc}(nominal)	1200 V
J_m	0.0887 Kg.m^2
B	0.00478 N.m./rad./s.
DC bus capacitor	6×10000μF
Nominal mechanical output power of turbine, at V_w =12 m/s , ρ = 1.25 Kg./m^2.	9×10^6 W

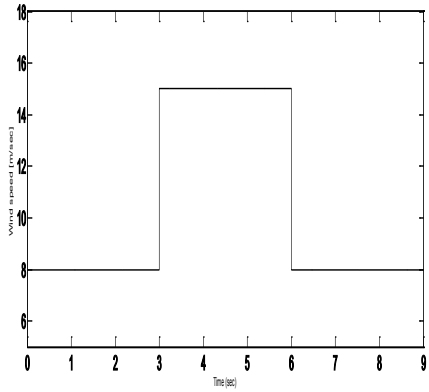

(a) Wind speed variation (m/sec)

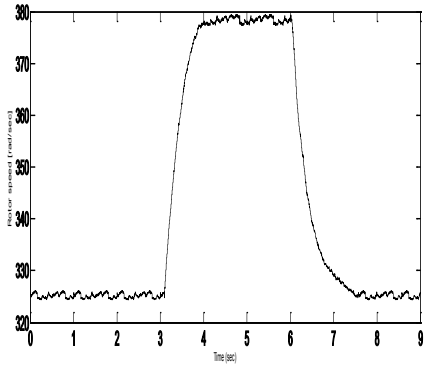

(b) Rotor speed (rad./sec.

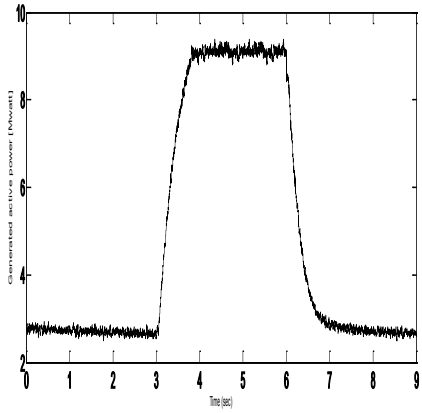

(c) Generated active power (Mwatt)

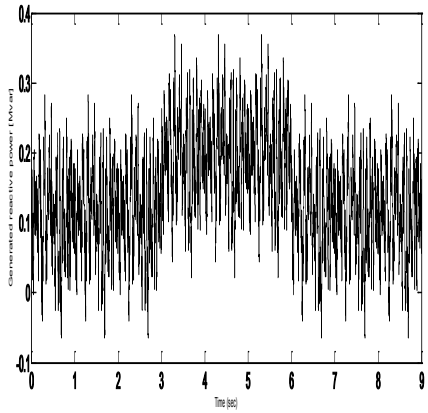

(d) Generated reactive power (Mvar)

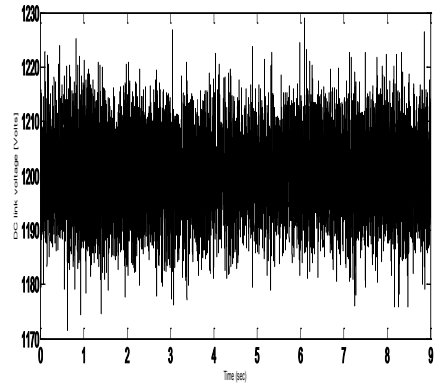

(e) DC Link voltage (Volts)

Fig.5: Performance of the proposed DFIG driven by a wind turbine system with wind speed step change.

The transient performance of the proposed scheme for a step change of wind speed from 8 m/sec to 15 m/sec in bi-directional is investigated as shown in fig.5. This figure shows that the proposed system exhibits good dynamic performance during wind speed transients. Fig.5.b shows that the values of rotor speed can be effectively calculated and have the same track as

the wind speed. The calculated values of generated active and reactive powers give the desired performance as shown in figs. 5.c and 5.d. The calculated values of dc link voltage are almost constant during the application and removal of the rated wind speed (15 m/sec) as illustrated in fig.5.e.

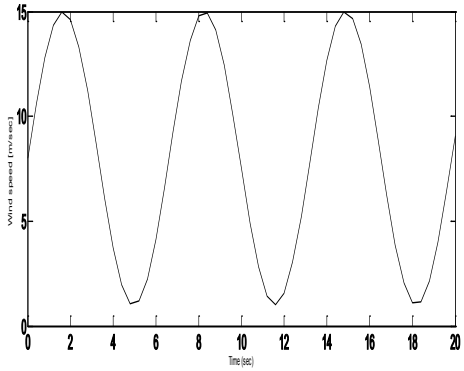

(a) Wind speed variation (m/sec)

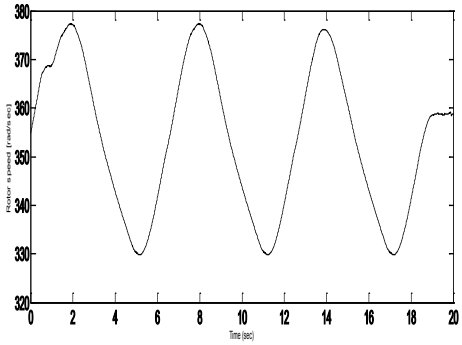

(b) Rotor speed (rad./sec.)

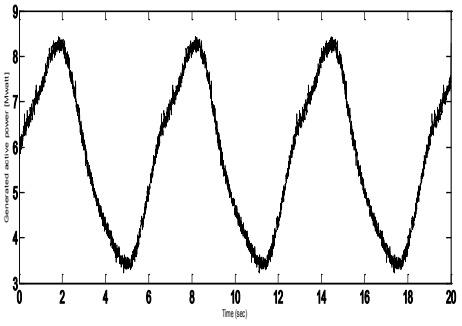

(c) Generated active power (Mwatt)

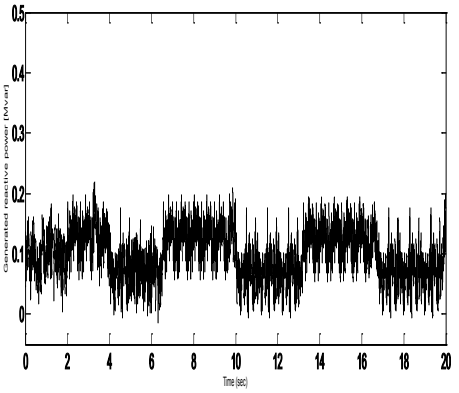

(d) Generated reactive power (Mvar)

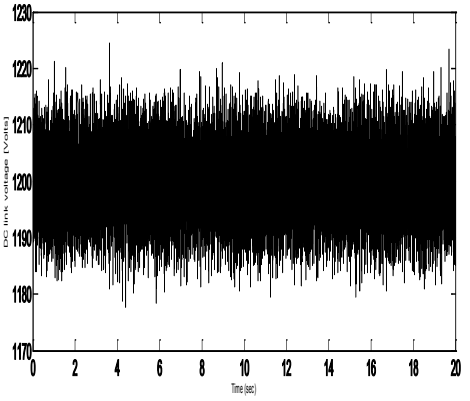

(e) DC Link voltage (Volts)

Fig.6: Dynamic response of the proposed system with sinusoidal variation of wind speed

The transient behavior of the proposed scheme is evaluated for sinusoidal variation of wind speed. The calculated values of rotor speed have the same profile of the wind speed as shown in fig.6.b. The calculated values of generated active and reactive powers have good matching with the sinusoidal variation of wind speeds as shown in figs. 6.c and 6.d. Fig.6.e illustrates that, the calculated values of the dc link voltage have constant values despite of the sinusoidal variation of wind speed. Moreover, this

voltage exhibits large amplitude of pulsations due to voltage source inverter PWM.

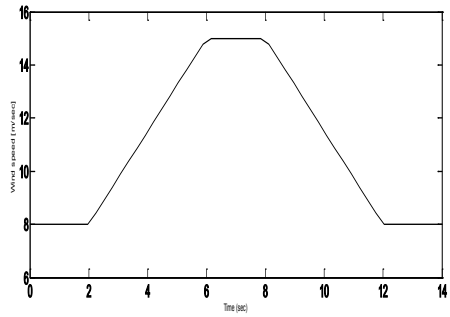

(a) Wind speed variation (m/sec)

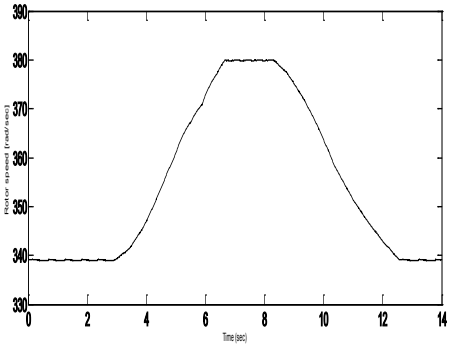

(b) Rotor speed (rad./sec)

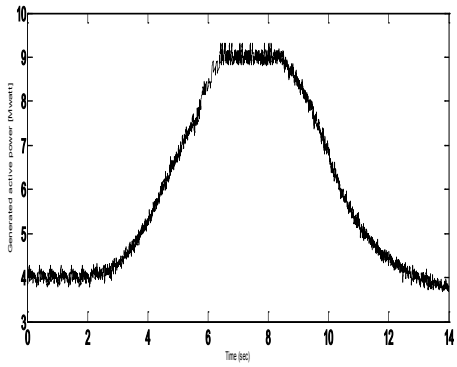

(c)Generated active power(Mwatt)

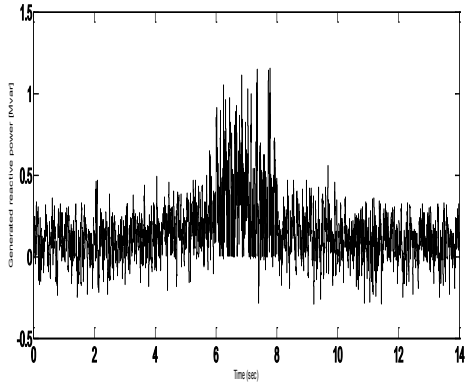

(d) Generated reactive power (Mvar)

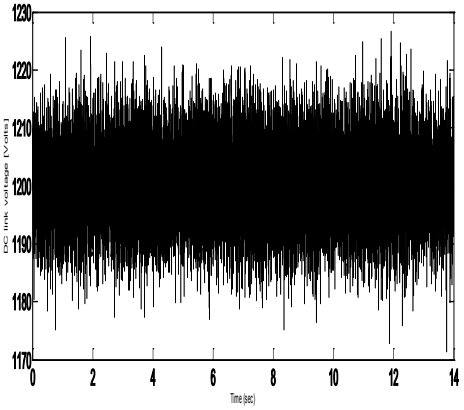

(e) DC Link voltage (Volts)

Fig.7: Performance of the proposed DFIG driven by a wind turbine system with linear bi-directional variation of wind speed

The transient performance of the proposed scheme has been tested for a change of wind speed in linear fashion. Thus, the wind speed is assumed to vary linearly from 8 m/sec. to 15 m/sec. in bi-directional. Figs. 7.a, 7.b, 7.c, 7.d and 9.e show the wind speed, actual rotor speed, the generated active power, the generated reactive power and the dc link voltage. Fig.7.b shows that the rotor speed has the same track as the wind speed with the proposed scheme. Fig.7.c indicates that the

generated active power matches the variation of the wind speed with fast and precise transient response. It is worthy to mention that the generated reactive power and the dc link voltage are kept constant during the change of wind speed as shown in Figs. 7.d and 7.e. However, the generated active and reactive powers and the dc link voltage exhibit high-frequency pulsation of large magnitude due to voltage source inverter PWM.

8 Conclusion

In this paper, a field orientation control scheme has been developed to control both rotor side and line side converters for a wind driven DFIG system. The proposed system consists of a wind turbine that drives a doubly fed induction generator connected to the utility grid through AC-DC-AC link. Field orientation method allows decoupled or independent control of both active and reactive power of the DFIG. This method is based on the theory of controlling the d^e and q^e axes components of voltage or current in rotating reference frames, using PI controllers for operating at maximum available wind power.

The dynamic model of the complete proposed system has been described. Computer simulation has been carried out in order to validate the effectiveness of the proposed system. The main conclusions that can be inferred from the present results are summarized as follows:

1- The transient performance of the proposed scheme is presented for a step change of wind speed. Fast and good response of the rotor speed, active and reactive powers are achieved following the application and removal of wind speed disturbance. In addition the dc link voltage is kept constant during the wind speed disturbance.
2- Simulation results demonstrate that the proposed system is capable of working through sinusoidal variations of wind speed and exhibits very good dynamic performance.
3- The dynamic performance of the proposed system has been investigated when the wind speed is changed linearly. The calculated values of rotor speed, active and reactive powers have good matching with wind speed variation. The results prove that, significant improvements of dynamic performance have been achieved.

References:

[1] A. Rasmussens, BTM Consults (2005), *International Wind Energy Development –World Market Update 2005, Forecast*. Ringkøbing, Denmark, (2006) pp. 2006-2010.

[2] Chowdhury Badrul H, Chellapilla Srinivas, "Double-fed induction generator control for variablespeed wind power generation" *Electric Power Systems Research* 76 (2006) , pp. 786-800

[3] E. Muljadi, K. Pierce, P. Migliore, "Control strategy for variable speed stall regulated wind turbines", *American Control Conference*, vol. 3,

24–26 June, (1998), pp. 1710-1714.

[4] E. Muljadi, C.P. Butterfield, "Pitch-controlled variable speed wind turbine Generation", *IEEE Trans. Ind.* Appl. 37 (1) (2001) pp. 240-246.

[5] Hany M. Jabr, Narayan C. Kar, "Fuzzy Gain Tuner for Vector Control of Doubly-Fed Wind Driven Induction Generator", *IEEE CCECE/CCGEI, Ottawa,* 1-4244-0038-4(2006), pp.2266-2269.

[6] R. Spee, S. Bhowmik and J. H. R. Enslin, "Novel control strategies for variable-speed doubly fed wind power generation systems," Renewable Energy, vol. 6 (1995), pp. 907–915.

[7] R. S. Pena, J. C. Clare and G. M. Asher, "Doubly fed induction generator using back-to-back PWM converters and its application to variable-speed wind-energy generation", *IEE Proc. Electric Power Applications,* vol. 143, No. 3, (1996), pp. 231-341.

[8] A. Tapia, G. Tapia, J.X. Ostolaza and J.R. Senz, "Modeling and control of a wind turbine driven doubly fed induction generator," *IEEE Trans. on Energy Conversion,* vol. 18(2003), pp.194-204.

[9] Lie Xu , "Coordinated Control of DFIG's Rotor and Grid Side Converters During Network Unbalance" *IEEE Trans. Power Electronics,* vol. 23, No. 3, MAY (2008), pp.1041-1049.

[10] Balasubramaniam Babypriya, Rajapalan Anita, "Modelling, Simulation and Analysis of Doubly Fed Induction Generator for Wind Turbines" *Journal of Electrical Engineering,* vol. 60, No. 2, (2009), pp.79–85.

[11] Hopfensperger, B. Atkinson, D. Lakin, R. A, "Stator Flux Oriented Control of a Cascaded Doubly-Fed Induction Machine", *IEE Proc. Electr. Power Appl.* 146 No. 6, (Nov1999), pp.597–605.

[12] Koch, F. W. , Erlich, I. Shewarega, F. "Dynamic Simulation of Large Wind Farms Integrated in A Multi Machine Network", *in Proceedings of 2003 IEEE PES General Meeting, Toronto, Canada,* (July 13–17 2003).

[13] MULLER, S. Deicke, M. De Doncker, R. W. "Doubly Fed Induction Generator Systems for Wind Turbines", *IEEE Industry Applications Magazine* 8 No. 3, (May/June 2002), pp. 26–33.

[14] Chee-Mun. Ong", *Dynamic Simulation Of Electronic Machinary using Matlab/Simulink"*, PRINTICE HALL, (1998).

[15] Pete. Vas ", *Vector Control Of AC Machines*",Oxford University , UK.

[16] P.C. Krause, O. Wasynzuk, S.D. Sudhoff, "*Analysis of ElectricMachineryand Drive Systems"*, IEEE press, (2002).

[17] P. Vas, "*Vector Control of AC Machines",* New York, Oxford Univ. Press,UK, (1990).

[18] R. Pena, J.C. Clare, G.M. Asher, "Doubly fed induction generator using back-to-back

PWM converters and its application to variable-speed wind-energy generation", *IEEE Proc.-Electr. Power Appl.*, Vol. 143, No. 3, (May 1996).

[19] Siegfried Heier, *"Grid Integration of Wind Energy Conversion Systems"*, ISBN 0-471-97143- X, John Wiley & Sons Ltd, (1998).